Phylogenomics of Thecamoebida (Discosea, Amoebozoa) with the Description of Stratorugosa tubuloviscum gen. nov. sp. nov., a Freshwater Amoeba with a Perinuclear MTOC

Article *in* Protist · October 2018

DOI: 10.1016/j.protis.2018.09.002

CITATIONS
0

READS
18

5 authors, including:

James Melton
University of Alabama
10 PUBLICATIONS **50** CITATIONS
SEE PROFILE

Fiona Wood
Georgia Institute of Technology
16 PUBLICATIONS **8** CITATIONS
SEE PROFILE

Mandakini Singla
Spelman College
23 PUBLICATIONS **17** CITATIONS
SEE PROFILE

Yonas Tekle
Spelman College
67 PUBLICATIONS **780** CITATIONS
SEE PROFILE

Protist, Vol. 170, 8–20, xx 2019
http://www.elsevier.de/protis
Published online date 16 October 2018

Protist

ORIGINAL PAPER

Phylogenomics of Thecamoebida (Discosea, Amoebozoa) with the Description of *Stratorugosa tubuloviscum* gen. nov. sp. nov., a Freshwater Amoeba with a Perinuclear MTOC

James T. Melton III[1], **Fiona C. Wood**, **Jordan Branch**, **Mandakini Singla**, and **Yonas I. Tekle**

Spelman College, 350 Spelman Lane Southwest, Atlanta, GA 30314, USA

Submitted March 19, 2018; Accepted September 18, 2018
Monitoring Editor: Sandra L. Baldauf

Thecamoebida Smirnov and Cavalier-Smith, 2011 (Discosea, Amoebozoa) has been molecularly understudied. The group until recently consisted of three genera containing species that live in terrestrial or aquatic environments. Here, we describe a fourth genus, *Stratorugosa tubuloviscum* gen. nov. sp. nov., which was isolated from a freshwater *Amoeba proteus* Ward's Science culture. Although this species most closely morphologically resembles a large, rugose *Thecamoeba*, *S. tubuloviscum* gen. nov. sp. nov. can be differentiated from *Thecamoeba* spp. by the following: 1) the presence of definitive finger-like (lobate-like) subpseudopodia extending at both the anterior and lateral parts of the cell during locomotion; 2) a peculiar locomotive mechanism with two sections, frontal and back, of the cells moving in a pulling and piggyback movement, respectively; 3) the presence of fibrillar cytoplasmic microtubules (MTs) organized by a prominent, perinuclear microtubule-organizing center (MTOC). A phylogenomic analysis of 511 genes assembled from transcriptomic data showed that this new genus was highly supported as sister to *Stenamoeba*. Despite the variance in gross morphology, *Stenamoeba* and *S. tubuloviscum* gen nov. sp. nov. both have MTOCs unlike two *Thecamoeba* spp., which display dot-like cytoplasmic MTs and lack an MTOC.

Key words: Amoebozoa; Thecamoebidae; phylogenomics; transcriptome; new genus; new species.

[1]Corresponding author.
e-mail jmelton@spelman.edu (J.T. Melton III).

Abbreviations: ICC, Immunocytochemistry; MT, microtubules; MTOC, microtubule-organizing center; OG, orthologous group; SSU, small subunit rDNA (18S).

https://doi.org/10.1016/j.protis.2018.09.002

Introduction

The amoebozoan family Thecamoebidae was originally described by Schaeffer (1926) for naked amoebae with ovoid to circular shapes that lacked pseudopodial extensions and for the most part maintained a consistent shape. This group has gone through several taxonomic expansions and contractions, and has been understudied in molecular studies. Schaeffer (1926) originally included two genera in this family, *Thecamoeba* and *Rugipes*. The type species of the latter (*R. bilzi* Schaeffer, 1926) is now considered to be a taxonomic synonym of *Thecamoeba* (Page 1969, 1971), and other members of this genus, *R. vivax* Schaeffer, 1926 and *R. placidus* Page, 1968, have now been moved to separate vannellid genera (i.e., *Clydonella* in Sawyer (1975) and *Vannella* in Bovee (1965), respectively). More recently, this family used to be comprised of eight genera of naked amoebae with a pellicle-like cell coat that are morphologically diverse (i.e., striate, rugose, lingulate, and polytactic morphotypes) (Page 1987, 1988; Smirnov et al. 2011). These genera included *Thecamoeba* Fromentel, 1874; *Sappinia* Dangeard, 1896; *Stenamoeba* Smirnov, Nassonova, Chao, et Cavalier-Smith, 2007; *Dermamoeba* Page et Blakey, 1979; *Paradermamoeba* Smirnov et Goodkov, 1996; *Parvamoeba* Rogerson, 1993*; Pseudothecamoeba* Page, 1988; and *Thecochaos* Page, 1981.

Increasing amounts of molecular data and morphological characters are continuing to shape our knowledge of this group. A closer examination of this taxon resulted in major taxonomic revisions (see Smirnov et al. 2011). These revisions include the transfer of genera previously placed within the Thecamoebidae into other taxonomic groups (i.e., *Dermamoeba* and *Paradermamoeba* to Dermamoebidae; *Parvamoeba* to Himatismenida- taxonomic revision made based on SSU and actin trees from Kudryavtsev et al. (2011)) or have been placed as incertae sedis due to the high degree of variation in morphology from the core thecamoebids and lack of molecular data (i.e., the polytactic genera *Pseudothecamoeba* and *Thecochaos* placed as incertae sedis in Smirnov et al. 2005) (Smirnov et al. 2011). Only three core genera (i.e., *Thecamoeba*, *Sappinia*, and *Stenamoeba*) have remained in the family Thecamoebidae prior to this study (Smirnov et al. 2011). *Stenamoeba stenopodia* (previously *Platyamoeba stenopodia* in Page 1969) was originally identified as a vannellid amoeba; however, SSU data showed that this isolate clustered within the Thecamoebidae (Smirnov et al. 2007). These three genera of Thecamoebidae are characterized by striate, rugose, and lingulate morphologies (morphotypes sensu Smirnov and Goodkov 1999; Smirnov and Brown 2004). Species in this group mostly have a thin, electron-dense cell coat and often have a glycocalyx layer (Dyková et al. 2010; Geisen et al. 2014; Goodfellow et al. 1974; Page and Blakey 1979; Smirnov et al. 2011; Wylezich et al. 2015) that sometimes has glycostyle-like structures (as observed in *Sappinia diploidea*; Michel et al. 2006).

The monophyly of *Thecamoeba*, *Sappinia*, and *Stenamoeba* has been supported by phylogenetic analyses based on SSU-rDNA (18S) (Michel et al. 2006; Pawlowski and Burki 2009; Shadwick et al. 2009; Smirnov et al. 2007; Tekle et al. 2008), a concatenation of SSU and actin genes (Lahr et al. 2011), and phylogenomics with transcriptome data (Kang et al. 2017). This clade has been defined using the name of the order, Thecamoebida (Adl et al. 2005, 2012; Kang et al. 2017), which will be used hereafter. Our recent phylogenomic studies reported that Thecamoebida forms a strong affiliation to a robust clade Flabellinea (Dactylopodida + Vannellida) (Tekle et al. 2016; Tekle and Wood 2017); however, Thecamoebida in these studies also included the unstable taxon *Vermistella* with poor support and lacked *Sappinia* in the phylogenetic analysis. This finding is contrary to previous classifications of Thecamoebida within Longamoebia (Dermamoebida + Thecamoebida + Centramoebida) – a lineage that included flat amoebae with pointed subpseudopodia and elongated cell shape (Smirnov et al. 2011). The monophyly of Longamoebia was questioned in our most recent phylogenomic studies (Tekle and Wood 2017). Similarly, another phylogenomic analysis with increased taxon sampling also corroborates our findings and placed the Thecamoebida within the Flabellinia (Kang et al. 2017).

Thecamoebida contains species that live in freshwater, marine, and terrestrial environments (e.g., Brown et al. 2007; Geisen et al. 2014; Kudryavtsev and Hausmann 2009; Michel et al. 2012; Page 1977, 1983, 1988). Some species are potentially pathogenic to humans causing amoebic encephalitis (*Sappinia diploidea* in Gelman et al. 2001; Gelman et al. 2003) and to other animals including fishes (*Thecamoeba hoffmani* in Sawyer et al. 1974; two species of *Stenamoeba*, *S. amazonica* and *S. limacina*, in Dyková et al. 2010) and horses (*Stenamoeba polymorpha* in Peglar et al. 2016). Historically, over 20 *Thecamoeba* species have been described. This genus currently

contains 11 species that are accepted taxonomically (combined from Page 1983, 1988; Smirnov and Goodkov 1999; Kudryavtsev and Hausmann 2009). These species have either a rugose or a striated morphology and a pellicle-like cell coat (Page and Blakey 1979; Page 1988; Smirnov and Goodkov 1999; Smirnov et al. 2011). *Thecamoeba* species range in length from as small as 11 μm (*T. orbis* Schaeffer, 1926 (Page 1977)) to as large as over 150 μm (*T. terricola* Greeff, 1866 (Page 1977)). There are currently only three known species of *Sappinia* Dangaerd, 1986 that exhibit rugose, striate (Smirnov et al. 2011), and lingulate (Wylezich et al. 2015) morphologies and are bi- to tetranucleate (Brown et al. 2007; Michel et al. 2006; Wylezich et al. 2015). These cells range in length from 35–85 μm as observed in *S. pedata* (Brown et al. 2007). Six lingulate and sometimes striate species are currently accepted taxonomically for *Stenamoeba* Smirnov, Nassova, Chao et Cavalier-Smith, 2007 (Page 1969 as *Platyamoeba stenopodia*; Dyková et al. 2010; Geisen et al. 2014; Peglar et al. 2016; Smirnov et al. 2007), and are the smallest thecamoebid cells ranging from 10.1 μm to 36 μm in *S. limacina* (Dyková et al. 2010).

Our limited knowledge of the Thecamoebida based on molecular data provides further reason to explore the diversity and phylogeny of this group. Here, we describe a fourth thecamoebid genus, *Stratorugosa tubuloviscum* gen. nov. sp. nov., based on morphological, cytological, ultrastructural, and large-scale phylogenomic evidence. The sample was isolated from an *Amoeba proteus* Ward's Science culture, indicating that such cultures might be good untapped sources of microbial diversity.

Results

Taxonomic Appendix Based on Adl et al. (2012)

Amoebozoa Lühe 1913 emend. Cavalier-Smith, 1998

•Discosea Cavalier-Smith 2004 sensu Kang et al. 2017

••Flabellinia Smirnov et al., 2005 sensu Kang et al. 2017

•••Thecamoebida Smirnov and Cavalier-Smith, 2011

Stratorugosa Melton et Tekle, n. gen.

DIAGNOSIS: Flattened flabellate amoebae forming lobate subpseudopodia. During locomotion, the uroidal part of the cell is dragged forward. Contains a perinuclear MTOC, and microtubules wrap around the nucleus.

TYPE SPECIES: *Stratorugosa tubuloviscum* Melton et Tekle

ETYMOLOGY: The name was derived from Latin in two parts; "stratum" meaning "layer" and "rugosa" meaning "wrinkled".

Stratorugosa tubuloviscum Melton et Tekle, n. sp.

DIAGNOSIS: Cells rugose and sometimes striate. Cells broadly fan-shaped, triangular, to spatulate during locomotion. A knob-shaped or elongated uroid frequently present while moving. Cells changing direction bi- to tri-lobate. Lobose or finger-like subpseudopodia sometimes present at anterior or posterior positions. Average locomotive cell sizes 89.8 μm (range from 47.5 μm to 134.9 μm) in length and 72.6 μm (range from 34.7 μm to 122.1 μm) in width. Floating cells with many radiating pseudopodia up to 60 μm in length. Cells uninucleate (average: 10.6 μm; range: 8.5 μm to 13 μm; oval to round in shape) with a single, central and spherical to oval-shaped nucleolus under the light microscope (average 6.5 μm; range: 5.5 μm to 7.9 μm); the nucleolus was never fragmented in pieces. MTs fibrillar, organized in a prominent, perinuclear MTOC always juxtaposed directly behind the nucleus, wrapped around the nucleus, and never extend throughout the whole granuloplasm or into the hyaloplasm.

HOLOTYPE: A live culture will be submitted to the American Type Culture Collection. Transcriptome data (raw reads) were submitted to NCBI's Sequence Read Archive (SRA) database (SRX4061347).

TYPE LOCALITY: Exact type locality is unknown as this sample came from a freshwater *Amoeba proteus* Ward's Scientific Culture.

ETYMOLOGY: The name is based on the "mistletoe-like" organization of the microtubules wrapping around the nucleus. The name is derived from Latin in two parts; "tubulo" meaning "tube" referring to the microtubules and "viscum" meaning "mistletoe".

DIFFERENTIAL DIAGNOSIS: While this amoeba most closely resembles a slow moving, rugose *Thecamoeba*, it can be differentiated from *Thecamoeba* species by the presence of fibrillar MTs and an MTOC, its broad fan shape and anterior and posterior lobose or finger-like subpseudopodia during locomotion, and a peculiar locomotive

mechanism with two sections, front and back (uroidal), of the cells moving in a pulling and piggyback movement, respectively.

Light Microscopy

Observed amoebae in Petri dishes with a medium of bottled water and rice infusion were adhered to the bottom of the Petri dish, attached to bacterial mats, or sometimes free-floating in the liquid medium (Supplementary Material Videos S1-2). The amoebae grew well on bacteria alone; however, they were voracious predators of other microbial eukaryotes in the original culture that UK-YT01 was isolated from. The attached amoebae were frequently observed in their locomotive forms and displayed a wide range of shapes and sizes (Figs 1, 2). This species most commonly had a rugose morphology and sometimes displayed dorsal striations or lateral wrinkles or ridges (Figs 1A, B, C, I; 2C, D). During locomotion, these amoebae can also be broadly fan-shaped where the cells have a greater width than length (Figs 1D, E; 2C, D).

A measurement of 100 cells showed that the average length of this species (89.8 μm) was greater than its average width (72.6 μm). The cells range in length from 47.5 μm to 134.9 μm and from 34.7 μm to 122.1 μm in width. The nucleus of the cell was oval to almost spherical in shape and averaged 10.6 μm in size (range: 8.5 μm to 13.0 μm). The nucleolus was always centrally located in a single spherical or oval shape that averaged 6.5 μm (range: 5.5 to 7.9 μm; Figs 1K; 2B, D). The average size of the hyaloplasm was 8.0 μm, and it ranged from approximately 5.4 μm to up to 13.8 μm in rare and irregularly shaped cells (Figs 1A-G, I-L; 2C, D). One to three spherical contractile vacuoles were present in the majority of the amoebae at the posterior end (Figs 1A-D, H, I, K, L; 2A, B, D); however, the contractile vacuoles sometimes traveled towards the middle of the cell (Fig. 2D). The average size of these contractile vacuoles was 15.5 μm (range 9.9 μm to 20.5 μm).

The new isolate has a peculiar locomotive mechanism with two sections, frontal and back (uroidal), of the cells moving in a pulling and piggyback motion, respectively (Supplementary Material Videos S1-2). In locomotive cells the amoeba has a fan shape leading with a flat, clear hyaloplasm in an anterolateral crescent. The leading hyaloplasm moves in a smooth and continuous manner at times forming pointed or finger-shaped subspeudopodia (Fig. 1G) that anastomose upon contact (Supplementary Material Video S1-2). There are several layers (1-5) of membrane folds on the top of the leading frontal hyaloplasm giving it the appearance of rugose or multilayered forms (Figs 1A, C; 2A, C). Some of these layers form pointed or finger shaped subpseudopodia usually facing in the direction of locomotion (Figs 1A, C, G; 2A, B).

The second section consists of the uroidal part of the cell, including the contractile vacuole, which is usually located near the middle of this section in the fully extended fan-shaped, actively moving amoebae (Fig. 1A-D, I, K, L). For the most part, the uroidal section does not seem to be completely attached to the surface; it is made of compact, bag-like membrane filled with cytoplasmic content (Supplemental Material Videos S1-2). During active locomotion, this section of the cell is shown to be dragged forward by the moving frontal section. During this pulling forward motion, the cytoplasmic content is observed into the leading, flattened part of the cell, creating a jerky type of movement of the uroidal section. A similar mechanism is also observed in amoebae in non-directional movement (Supplementary Material Videos S1-2). The amoebae are sometimes observed to form bi- (Figs 1F; 2A) to tri-lobed (Fig. 2B) shapes of roughly equal parts of the cell connected by the uroidal section. During directional movement, these two to three lobes merge (fuse) to form a continuous fan-shaped amoeba (Supplementary Material Videos S1-2).

ICC and Confocal Imaging

The microtubules, DNA, and plasma membrane were stained in the UK-YT01 isolate. The cell mask allowed for a better visualization of cell boundaries and the subpseudopodia (Fig. 3A, C, E, F). The cytoplasmic microtubules (MTs) were present in networks of fibers (Fig. 3A-E). The MTs were organized by a prominent microtubule-organizing center (MTOC) that was closely associated with the oval or spherical shaped nucleus typically located slightly posterior to the middle of the cell (Fig. 3A-C). The MTOC was mostly observed on top of the nucleus (facing the posterior end) forming a visible central ring, where all of the MTs originate (Fig. 3A-C). The majority of the MTs originating from the MTOC were observed to tightly wrap around the nucleus (Fig. 3A-C). Other MTs originating from the MTOC are also observed to branch out in different directions, but mostly extend back into the posterior section of the cell (Fig. 3A-E). Very few microtubules extended forward throughout a large portion of the granuloplasm, and were not observed to extend in to the hyaloplasm. Loose MT fibers were examined around the edges of some of the

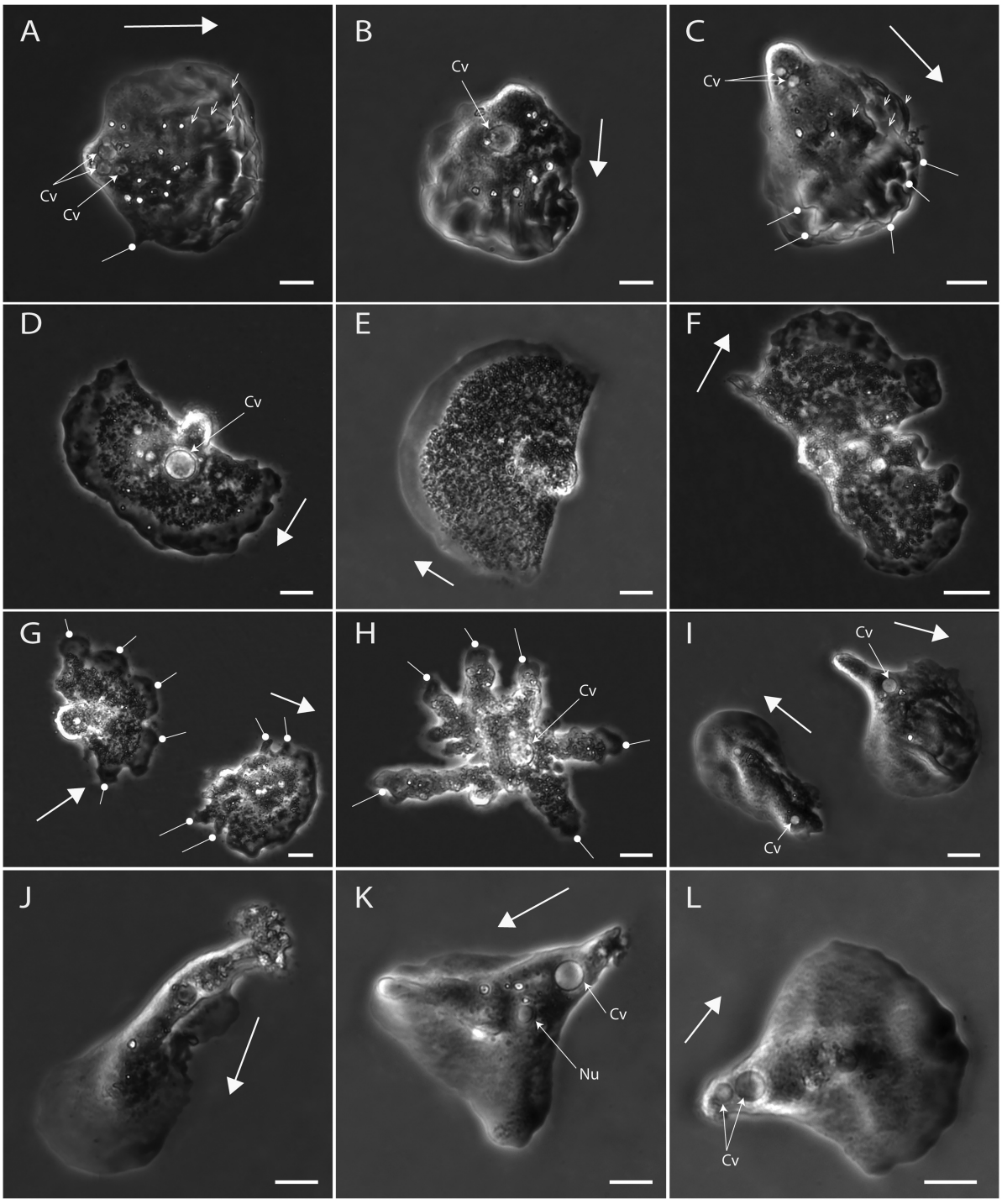

Figure 1. Light microscope images of *Stratorugosa tubuloviscum* gen. nov. sp. nov. The solid, open, and circular-shaped arrows are pointing in the direction of movement, layers, and subpseudopodia, respectively. Contractile vacuoles (Cv) and nucleus (Nu) are labeled in the images. A) the most common morphology of this species: a fan-shaped, rugose amoeba showing approximately five cascading layers of the amoeba, three contractile vacuoles at the posterior end, and refractile inclusions. **B**) a rugose amoeba with one contractile vacuole at the uroidal end and longitudinal wrinkles. **C**) a rugose amoeba with displaying several layers and pseudopodia. **D**) a broadly fan-shaped amoeba with a large contractile vacuole. E) a broad

cells, but this might be a fixation artifact since they were not continuous with the rest of the MTs originating from the perinuclear MTOC (Fig. 3E).

Transmission Electron Microscopy (TEM)

TEM micrographs were taken of the nucleus, food vacuoles, plasma membrane, and mitochondria (Fig. 4). The images of the nucleus and nucleolus were elongated (bean-shaped) with an irregular outline (Fig. 4A-B). The nucleus was bounded with an electron dense nuclear membrane and contained a single non-homogeneous nucleolus with 5-6 round-shaped less electron dense patches (Fig. 4A, B). Membrane-bound food vacuoles often contained multiple bacteria (Fig. 4A). Most of the images of the bi-layered plasma membrane showed little to no extracellular cell coat-like materials (Fig. 4D, E). The plasma membrane was mostly smooth with no visible glycocalyx layer, but in some samples a very thin layer of an electron dense, amorphous cell coat was observed (Fig. 4D, E). The lack of a cell coat in our samples might indicate a suboptimal fixation protocol. The round-shaped mitochondria were tubulo-cristate, typically 0.5 μm to 1 μm in across (Fig. 4C).

Phylogenomic Analysis

The maximum likelihood phylogenomic analysis of the concatenated 511-gene amino acid dataset yielded a well-resolved and strongly supported Thecamoebida clade, both in the larger (Discosea, Fig. 5) and smaller (Flabellinia, Supplementary Material Fig. S1) taxon sampling analyses. In all of our analyses, the UK-YT01 isolate clustered closely with an undescribed species, Thecamoebida isolate RHP1-1 SRX2691210, with strong support (Fig. 5, Supplementary Material Fig. S1). The UK-YT01 + Thecamoebida isolate RHP1-1 clade was sister to a clade of *Stenamoeba* species with a moderate bootstrap support (80%, Fig. 5). This sister group relationship was strongly supported (100% bootstrap) in the smaller taxon sampling analysis (Supplementary Material Fig. S1). *Thecamoeba* and *Sappinia* also formed a highly supported clade, which branched as sister to the clade consisting of ((UK-YT01+ Thecamoebida isolate RHP1-1 SRX2691210) + the genus *Stenamoeba*) with full support in both analyses (Fig. 5, Supplementary Material Fig. S1).

Pairwise Analysis of UK-YT01 and an Undescribed Thecamoebida Isolate RHP1-1

A reciprocal nucleotide blast of the eukaryotic contigs from the assembled transcriptomes of UK-YT01 and an undescribed Thecamoebida isolate RHP1-1 had 3,264 total hits. A pairwise analysis of these hits showed that a majority of the contigs (89%) were less than 2% divergent. A similar pattern of divergence in the transcriptomic data of conspecific isolates has been noted (Tekle and Wood, under review). A total of 1,092 of these contigs were 100% identical (33.19% of the contigs), and 1,640 contigs were less than 1% divergent (49.85%). A total of 11% of the contigs fell outside of 2% divergence might represent paralogs or other false hits due to the incomplete nature of transcriptome data. The pairwise alignment of the two SSU sequences (471 bps) of UK-YT01 and Thecamoebida isolate RHP1-1 were 99.8% identical (data not shown). This high sequence similarity provides further indication that these two isolates are likely conspecific. The SSU sequences were derived from transcriptome data and contained large insertions when compared to other thecamoebid SSU sequences. Therefore, these sequence data could not be reliably used for phylogenetic inference.

Discussion

Morphology

UK-YT01, here described as *Stratorugosa tubuloviscum* gen. nov. sp. nov, clearly represents a distinct new genus and species within the Thecamoebida based on morphological, cytological, ultrastructural evidences. *S. tubuloviscum* most often morphologically resembles slowly moving

fan-shaped amoeba with a clear distinction of the hyaloplasm and granuloplasm (image taken from glass slide). **F**) amoeba changing directions, cell is in two distinct parts. **G**) fan-shaped amoebae with lobose pseudopodia. **H**) floating amoeba with radiating pseudopodia up to 60 μm in length. **I**) a long rugose amoeba (left), and amoeba with a long trailing uroid and dorsal ridges or folds (right). **J**) amoeba with a long trailing uroid and large smooth hyaloplasm. **K**) triangular shaped amoeba with trailing uroid showing a contractile vacuole and the nucleus. **L**) amoeba spatulate with two posterior contractile vacuoles. All scale bars represent 20 μm and all images were taken on plastic Petri dishes with the exception of Figure 1E, which was taken on a glass slide.

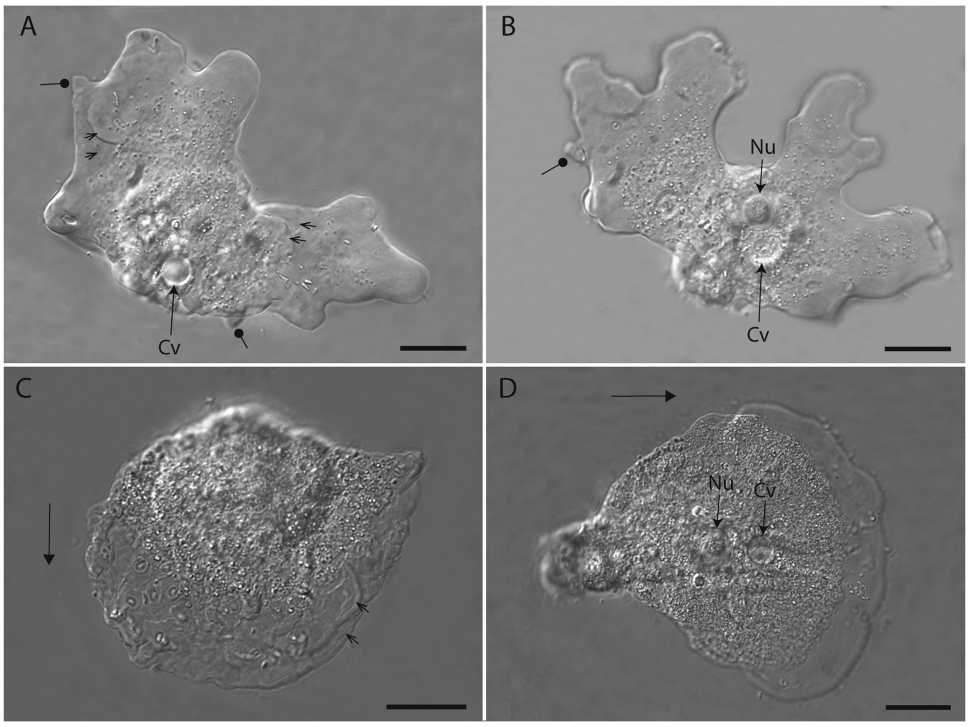

Figure 2. Light microscope images of *Stratorugosa tubuloviscum* taken with DIC on a glass slide. The solid arrow, open arrow, and diamond shaped arrow are pointing in the direction of movement, layers, and subpseudopodia, respectively. Contractile vacuoles (Cv) and nucleus (Nu) are labeled in the images. **A)** amoeba changing direction appearing bi-lobed with contractile vacuole present at posterior end. **B)** amoeba appearing tri-lobed with a clear oval-shaped nucleus and a central nucleolus. **C)** fan-shaped amoeba that is highly wrinkled in appearance. **D)** amoeba displaying two longitudinal dorsal wrinkles or ridges, two contractile vacuoles (one in the uroid section and the other located anterior to the nucleus), and a clearly defined hyaloplasm and granuloplasm that is typical of this species during locomotion. All scale bars represent 20 μm.

rugose members of *Thecamoeba* (Supplementary Material Table S1). While this species can be confused with a *Thecamoeba* species, the distinguishing characteristics for this new genus are the following: 1) the presence of pointed or finger-like (lobate-like) subpseudopodia in both the anterior and lateral positions of actively moving or loosely attached amoebae (Figs 1A, C, G; 2A, B), while *Thecamoeba* spp. lack definitive subpseudopodia from their main body during locomotion (Page 1977); 2) the jerky movements of the uroidal section of the cell as the moving frontal part of the cell drags the posterior end of the cell forward (Supplementary Videos S1-2), while the locomotion of *Thecamoeba* species has been described as “tractor-like” and is often smoother and acting in a single motion (Page 1977); 3) the presence of fibrillar MTs with a prominent, perinuclear MTOC (Fig. 3A-E), compared to *Thecamoeba* spp. dot-like cytoplasmic MTs (see fig. 1i in Tekle and Williams 2016). The new isolate can easily be discerned from the other two genera in Thecamoebida (i.e., *Sappinia* and *Stenamoeba*). *Sappinia* spp. are rugose and striate in morphology but have two to four nuclei (Brown et al. 2007; Michel et al. 2006; Wylezich et al. 2015), while *S. tubuloviscum* is uninucleate. *Stenamoeba* species are lingulate to ovoid or oblong in morphology (Dyková et al. 2010; Geisen et al. 2014; Peglar et al. 2016) compared to the broad fan-shaped cells of *S. tubuloviscum*.

Stratorugosa tubuloviscum exhibited fibrillar cytoplasmic MTs and a prominent, perinuclear MTOC (Fig. 3A-E). While a perinuclear MTOC is reported in other amoebae (e.g. *Dictyostelium* (Tekle and Williams 2016) and *Stereomyxa ramosa* ATCC® 50982™ (Tekle and Wood 2017)), there are noticeable differences in arrangement, distribution, and abundance of MTs originating from the MTOC in *S. tubuloviscum*. In *Stereomyxa ramosa* and *Dictyostelium*, the MTs originating from the perinuclear MTOC do not wrap around the nucleus; they are loosely packed (fewer in *Dictyostelium*) and fan out to the rest of the cell body or granuloplasm (Tekle and Williams 2016). Most MTs

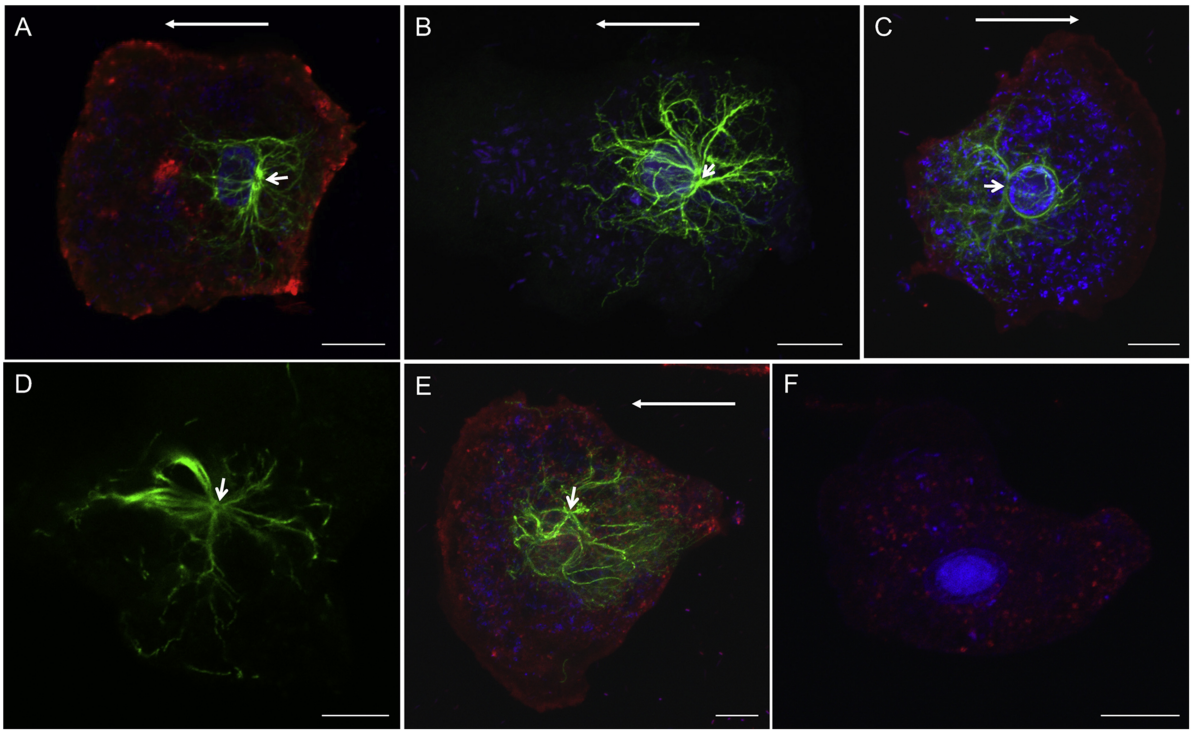

Figure 3. Confocal imaging of microtubules (green), DNA (blue), and the plasma membrane (red) in *Stratorugosa tubuloviscum* gen. nov. sp. nov. Cell shows MTs in a fibrillar network closely associated with the nucleus and a prominent MTOC (indicated by the open arrows). **A**) cell stained for microtubules, DNA, and the plasma membrane; shows a prominent MTOC juxtapose to the posterior portion of the oval-shaped nucleus; microtubules extend primarily backward into the uroidal part of the cell with few extending forward; microtubules not present throughout the granuloplasm or into the hyaloplasm; cell shows small lateral subpseudopodia. **B**) cell stained for microtubules and DNA; image shows the presence of an MTOC and the mistletoe-like appearance of the microtubules that wrap around the nucleus; microtubules are extending back into the uroidal portion of the cell with few extending forward. **C**) cell stained for microtubules, DNA, and the plasma membrane; microtubules shown wrapped around the outside of the nucleus and extending backward into the uroidal portion of the cell; very few microtubules extending forward; cell shows distinct lateral subpseudopodia. **D**) cell stained for microtubules; microtubules extending from a prominent MTOC in a ring-like structure. **E**) cell stained for microtubules, DNA and the plasma membrane; a less prominent MTOC is present in this cell; the microtubules are mostly present in the middle of the cell that extend backward toward the uroidal portion of the cell; loose microtubule filaments present toward the outside of the cell, which could potentially be due to fixation; cell shows lateral subpseudopodia. **F**) cell stained for DNA and the plasma membrane; image shows the clear distinction of the oval-shaped nucleus (fainter staining around the outside of the nucleus) and nucleolus (darker staining inside the nucleus). Scale bars are 11 μm.

originating from the perinuclear MTOC of *S. tubuloviscum* were tightly wrapped around the nucleus sometimes forming an intertwined fibrillar arrangement in the shape of a mistletoe (Fig. 3A-E). The MTOC has a clear ring-shaped center where most of the MTs seem to radiate from. This ring-like nucleation center was not evident in *Dictyostelium* or *Stereomyxa ramosa* (Tekle and Williams 2016; Tekle and Wood 2017). Similarly, the remaining MTs originating from the MTOC do not extend far from the nucleus unlike most in amoebae examined so far. The cytoplasmic MTs in most amoebae were observed to be distributed uniformly in the granuloplasm in a complex tightly packed network (*Cochliopodium*, Tekle and Williams 2016), parallel (members of Tubulinea), coiled (Centramoebida Tekle and Wood 2017), or dot-like (*Thecamoeba*, Tekle and Williams 2016). Other types of MTOCs not associated with the nucleus were also observed in *Cochliopodium* (Tekle and Williams 2016). *Stratorugosa tubuloviscum* adds a new variation of MTOC in Amoebozoa. Interestingly, a perinuclear MTOC has been reported in *Stenamoeba* (Geisen et al. 2014) as well as

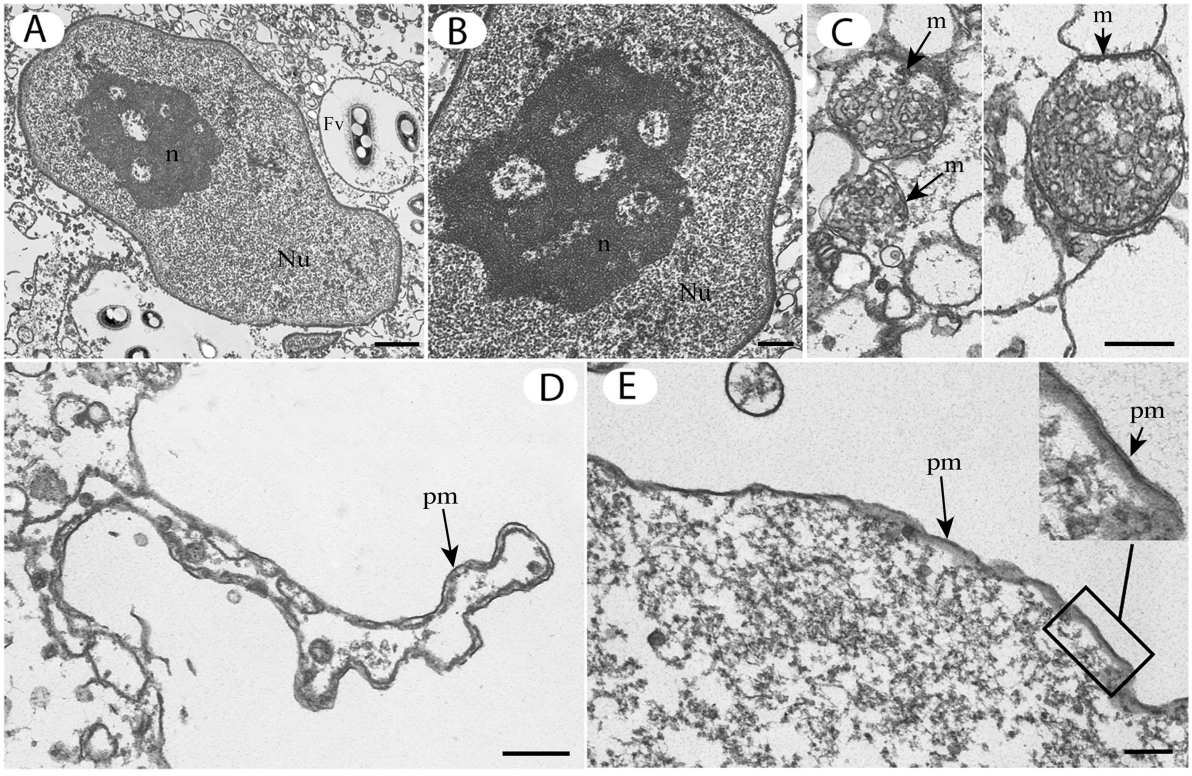

Figure 4. TEM micrographs of *Stratorugosa tubuloiscum* gen. nov. sp. nov. The letters indicate the following: Fv- food vacuole; m- mitochondrion; n- nucleolus; Nu- nucleus; pm- plasma membrane. **A**) micrograph of the slightly amorphous nucleus and nucleolus; the nucleus has a clear nuclear membrane; the non-homogeneous nucleolus has rounded edges and six gaps or holes present inside; one large gap is centrally located with the other gaps arranged around the central gap; to the right of the nucleus is a membrane bound food vacuole containing two bacterial cells; scale bar is 1 μm. **B**) micrograph of the slightly amorphous nucleus and nucleolus; nucleus contains a clear nuclear membrane; the non-homogeneous nucleolus has pointed and rounded edges with six total gaps; one of the gaps is centrally located with the other five gaps arranged in a circle around the central gap; scale bar is 500 nm. **C**) micrograph of the mitochondria with tubular cristae; scale bar is 500 nm. **D**) micrograph of the thin, amorphous plasma membrane with little to no cell coat or glycocalyx layer; scale bar is 500 nm. **E**) micrograph of the thin, amorphous plasma membrane with little to no glycocalyx layer; the inset shows an enlarged version of the plasma membrane; scale bar is 200 nm.

some microtubules near the nucleus in *Sappinia* (Wylezich et al. 2015) based on ultrastructural studies. Ultrastructural studies are not ideal for detecting the MTOC in amoeba cells. TEM studies report mixed results in the detection of an MTOC using this technique. MTOCs have been missed by only using TEM data (e.g., *Cochliopodium gallicum*; Kudryavtsev and Smirnov 2006), or MTOCs have been reported (e.g., *Cochliopodium spiniferum*; Kudryavtsev 2004), however, were not shown with ICC (Tekle and Williams 2016). However, if these reports are confirmed using similar ICC techniques used in this study in *Stenamoeba*, the nature of the MTOC could serve as a potential synapomorphy for the strong relationship of the new isolate and *Stenamoeba* observed in the phylogenomic analysis (Tekle and Williams 2016). The nature and presence of an MTOC has been found to be a useful taxonomic feature for defining groups such as *Cochliopodium* (Tekle and Williams 2016). These results demonstrate that features derived from cellular proteomic features such as MTs and MTOCs might be a useful synapomorphic character that could contribute to our understanding of Amoebozoa diversity (Geisen et al. 2014).

Members of Thecamoebida have been observed to have an amorphous cell coat with a thin glycocalyx layer as observed in *Thecamoeba* (Kudryavstev and Hausmann 2009; Page and Blakey 1979; Page 1991; Smirnov 1999; Smirnov et al. 2011), *Sappinia* (Goodfellow et al. 1974), and *Stenamoeba* (Dyková et al. 2010; Geisen et al. 2014; Peglar et al.

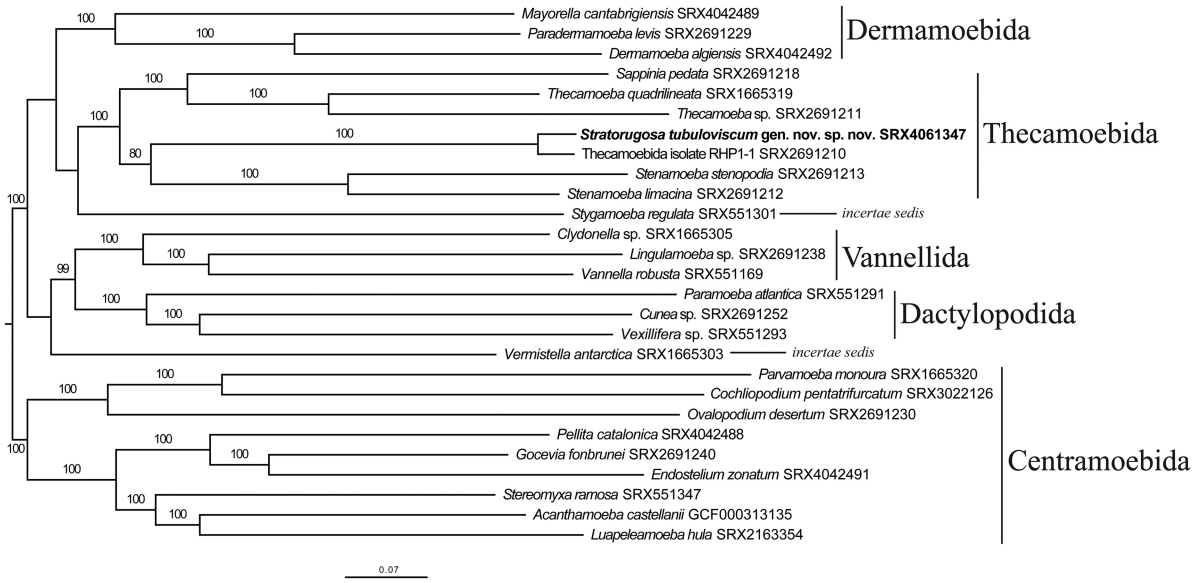

Figure 5. A maximum likelihood phylogenomic analysis of Discosea based on 106,983 amino acid characters showing the placement of *Stratorugosa tubuloviscum* gen. nov. sp. nov. This analysis was run using RAxML with the PROTGAMMALGF model of amino acid evolution and 1000 bootstrap replicates. Bootstrap values below 50% were removed.

2016), and sometimes have extra glycostyle-like structures in *Sappinia diploidea* (Michel et al. 2006; Smirnov et al. 2011). Page and Blakely (1979) suggested that the cell coat was useful for genus-level identifications and maybe some species level identifications in this group. Michel et al. (2006) observed different sizes of the cell coat of different strains of *Sappinia diploidea*, and also showed glycostyle-like structures, which were lacking in TEM images of Goodfellow et al. (1974). The cell coat of *Stratorugosa tubuloviscum* was thin and lacked any glycostyle-like structures. While the lack of detection of a cell coat in our isolate might be due to fixation problems, the morphology of the cell coat varies among the thecamoebids and presently does not appear to provide a defining characteristic suitable for most species level identifications within the Thecamoebida.

Phylogenomics of the Thecamoebida

Our phylogenetic analysis strongly supported the placement of *Stratorugosa tubuloviscum* gen. nov. sp. nov. within the clade Thecamoebida. Our results contrast with the main phylogenetic tree (i.e., fig. 3) from Kang et al. (2017), as their results showed that "Thecamoebida isolate RHP1-1", an isolate that is likely conspecific with our isolate, shared a more recent common ancestor with the *Thecamoeba* + *Sappinia* clade than with *Stenamoeba*. However, this relationship was not strongly supported (70% bootstrap). It is important to note that Thecamoebida isolate RHP1-1 and *Stenamoeba* formed a strongly supported clade in two supplemental phylogenomic trees (figs S1 and S2 from Kang et al. 2017). Differences in phylogenetic position are likely due to differences in methods such as model of amino acid evolution. Despite the variances in phylogenetic position of these two studies, it is apparent that our isolate and the isolate from Kang et al. (2017) are representatives of a new genus and species within the Thecamoebida.

Methods

Isolation and culturing: The sample of *Stratorugosa tubuloviscum* was isolated into a monoclonal culture (designated as UK-YT01) from an *Amoeba proteus* culture purchased from the Ward's Science live culture collections (Item number 470176-570). These two amoebae and other microbial eukaryotes were inhabiting this culture in a medium of distilled water and rice grains. After isolation, the culture was kept at room temperature in plastic Petri dishes (100 mm × 15 mm) with bottled natural spring water (Deer Park ®; Nestle Corp., Glendale, CA) and autoclaved rice grains for bacterial growth for food. The type specimen will be deposited at ATCC.

Microscopy: A morphological analysis was performed on Zeiss Axiovert 40 CFL and Nikon Eclipse E1000 (with DIC) compound light microscopes, and images were taken with a Zeiss AxioCam ICm 1 camera. Measurements of the length and width, contractile vacuoles, hyaloplasm, and nucleus were made in ZEN 2012 lite.

Immunocytochemistry (ICC) methods were used to stain microtubules (anti-alpha-tubulin monoclonal antibody), DNA (DAPI), and the plasma membrane (CellMask™ Orange, Life Technologies). The amoeba was grown in two-well glass cham-

ber slides (Thermo Scientific™, Nunc Lab-Tek, Rochester, NY) in the same bottled natural spring water and rice grains. ICC staining and confocal microscopy was performed following Tekle and Williams (2016).

For TEM, the samples were fixed and embedded in low viscosity epon following Tekle et al. (2015). Sectioning and TEM imaging was performed at Morehouse School of Medicine in Atlanta, GA.

Molecular data collection and analysis: Cells were collected from four 100 mm x 15 mm Petri dishes with good growth of the amoebae, and a pellet was made by centrifugation. A total of 9.83 ng/μl of RNA was extracted with the NucleoSpin® RNA kit (Macherey-Nagel, Düren, Germany) according to the manufacturer's protocol. The quantity of RNA was measured with a Qubit® RNA HS Assay Kit and a Qubit® 3.0 Fluorometer (Life Technologies, Carlsbad, CA). Double stranded cDNA was prepared using 2.375 μl of RNA with the Clontech SMART-Seq® v4 Ultra® Low Input RNA Kit (Takara Bio USA, Mountain View, CA, USA). This yielded 25.9 ng/μl of cDNA. A 1:100 dilution was made to bring the concentration to ~0.20 ng/μl, and 5 μl (1 ng total) was used for library preparation with the Nextera® XT DNA Library Preparation kit (Illumina In., San Diego, CA, USA). The resulting sample (5.0 ng/μl) was sent to Yale Center for Genomic Analysis (West Haven, CT) for sequencing on an Illumina HiSeq 2000 platform.

A total of 60.2 million paired end reads were retrieved. The raw reads were deposited to NCBI's SRA database (SRX4061347). Raw reads were trimmed with BBduk, which is a part of the BBMap package (Bushnell 2015; Joint Genome Institute, U.S. Department of Energy, Walnut Creek, CA, USA); 33.2 million reads were assembled with rnaSPAdes (Bankevich et al. 2012); and 12,602 contigs were filtered for eukaryotic contigs (5,279 contigs) by using the USEARCH algorithm (Edgar 2010) against a database of prokaryotic and eukaryotic sequences retrieved from Genbank.

Phylogenetic trees were made from two different datasets: one with representatives from across the Discosea clade and another with just Flabellinia. Taxon sampling and outgroups were based on the phylogeny of Kang et al. (2017), which was also followed for our taxonomic assignments in combination with Adl et al. (2012). For the Discosea phylogenetic analysis, we selected 15 members of the Flabellinia: six species of Thecamoebida (two *Thecamoeba*, two *Stenamoeba*, one *Sappinia*, and one unidentified Thecamoebida isolate (RHP1-1) that was collected from a freshwater pond near the campus of Mississippi State University in Starkville, MS, used in Kang et al. (2017), two species currently designated as *incertae sedis* (*Stygamoeba regulata* and *Vermistella antarctica*), and six outgroup species from Dactylopodida (*Cunea* sp., *Vexillifera* sp., and *Paramoeba atlantica*) and Vannellida (*Clydonella* sp., *Lingulamoeba* sp., and *Vannella robusta*), as well as the new isolate designated as UK-YT01. Additionally, 12 outgroup taxa were also selected from Centramoebia and Dermamoebida. The previously mentioned 15 members of Flabellinia were used for the Flabellinia only phylogenomic analysis. The contigs from the transcriptome assemblies of these taxa were mined for the 550 orthologous groups (OGs) used in previous phylogenomic analyses (Tekle et al. 2016; Tekle and Wood 2017) using blastp (Altschul et al. 1990). The best hit for each OG in each transcriptome was collected if it had an e-value below $1e^{-15}$. The collected sequences for each OG were kept only if UK-YT01 and at least one other transcriptome had positive hits; 511 OGs met these criteria. The sequences were then aligned using MAFFT (Katoh and Standley 2013) with default settings and then concatenated with a custom python script into the final supermatrix, which had a total of 171006 characters in the Discosea analysis and 168,802 characters in the Flabellinia-only analysis. The supermatrix was submitted to the Gblocks server (Castresana 2000; Talavera and Castresana 2007) with the least stringent option to extract alignment regions for phylogenomic analysis, resulting in a final alignment of 106,983 characters for the Discosea analysis and 111,416 amino acid characters for the Flabellinia analysis. Phylogenomic trees were then constructed using RAxML (Stamatakis et al. 2008) as implemented on the CIPRES Science Gateway (Miller et al. 2010), with PROTGAMMALGF model and 1000 bootstraps.

To investigate the close similarity between UK-YT01 and the Thecamoebida isolate from Kang et al. (2017), a reciprocal blastn search was performed on the assembled transcriptomes of the two species to recover putative orthologs. The pairwise distances between the orthologs were calculated using emboss's distmat function (Rice et al. 2000) to determine the average distance between the two species.

Acknowledgements

This work was supported by the National Science Foundation (NSF, USA) RIA Grant (1409587) and National Institutes of Health (NIH, USA) (1R15GM116103-01) to YIT. National Science Foundation HBCU-UP (1436759), a postdoctoral fellowship support, to JTM. We would like to thank Michael McGinnis and Lawrence Brako, for technical assistance with data collection and two anonymous reviewers for their helpful feedback. The authors are grateful to Prof. O. Roger Anderson for helpful discussions on the new isolate.

Appendix A. Supplementary data

Supplementary data associated with this article can be found, in the online version, at https://doi.org/10.1016/j.protis.2018.09.002.

References

Adl SM, Simpson AGB, Farmer MA, Andersen RA, Anderson OR, Barta JR, Bowser SS, Brugerolle G, Fensome RA, Fredericq S, James TY, Karpov S, Kugrens P, Krug J, Lane CE, Lewis LA, Lodge J, Lynn DH, Mann DG, McCourt RM, Mendoza L, Moestrup Ø, Mozley-Standridge SE, Nerad TA, Shearer CA, Smirnov AV, Spiegel FW, Taylor MFJR (2005) The new higher level classification of eukaryotes with emphasis on the taxonomy of protists. J Eukaryot Microbiol **52**:299–451

Adl SM, Simpson AG, Lane CE, Lukeš J, Bass D, Bowser SS, Brown M, Burki F, Dunthorn M, Hampl V, Heiss A, Hoppenrath M, Lara E, leGall L, Lynn DH, McManus H, Mitchell EAD, Mozley-Stanridge SE, Parfrey LW, Pawlowski J, Rueckert S, Shadwick L, Schoch C, Smirnov A, Spiegel FW (2012) The revised classification of eukaryotes. J Eukaryot Microbiol **59**:429–514

Altschul SF, Gish W, Miller W, Myers EW, Lipman DJ (1990) Basic local alignment search tool. J Mol Biol **215**:403–410

Bankevich A, Nurk S, Antipov D, Gurevich AA, Dvorkin M, Kulikov AS, Lesin VM, Nikolenko SI, Pham S, Prjibelski AD, Pyshkin AV, Sirotkin AV, Vyahhi N, Tesler G, Alekseyev MA, Pevzner PA (2012) SPAdes: a new genome assembly algorithm and its applications to single-cell sequencing. J Comput Biol **19**:455–477

Bovee EC (1965) An emendation of the ameba genus *Flabellula* and a description of *Vannella* gen. nov. Trans Am Micros Soc **84**:217–227

Brown MW, Spiegel FW, Silberman JD (2007) Amoeba at attention: phylogenetic affinity of *Sappinia pedata*. J Eukaryot Microbiol **54**:511–519

Bushnell B (2015) BBMap short-read aligner, and other bioinformatics tools, Retrieved from: source forge.net/projects/bbmap

Castresana J (2000) Selection of conserved blocks from multiple alignments for their use in phylogenetic analysis. Mol Biol Evol **17**:540–552

Dyková I, Kostka M, Pecková H (2010) Two new species of the genus *Stenamoeba* Smirnov, Nassonova, Chao et Cavalier-Smith, 2007. Acta Protozool **49**:245–251

Edgar RC (2010) Search and clustering orders of magnitude faster than BLAST. Bioinformatics **26**:2460–2461

Geisen S, Weinert J, Kudryavtsev A, Glotova A, Michael B, Smirnov A (2014) Two new species of the genus *Stenamoeba* (Discosea, Longamoebia): Cytoplasmic MTOC is present in one more amoebae lineage. Europ J Protistol **50**:153–165

Gelman BB, Popov V, Chaljub G, Nader R, Rauf SJ, Nauta HW, Visvesvara GS (2003) Neuropathological and ultrastructural features of amebic encephalitis caused by *Sappinia diploidea*. J Neuropathol Exp Neurol **62**:990–998

Gelman BB, Rauf SJ, Nader R, Popov V, Borkowski J, Chaljub G, Nauta HW, Visvesvara GS (2001) Amoebic encephalitis due to *Sappinia diploidea*. JAMA **285**:2450–2451

Goodfellow LP, Belcher JH, Page FC (1974) A light- and electron-microscopical study of *Sappinia diploidea*, a sexual amoeba. Protistologica **2**:207–216

Kang S, Tice AK, Spiegel FW, Silberman JD, Pánek T, Cepicka I, Kostka M, Kosakyan A, Alcântara DMC, Roger AJ, Shadwick LL, Smirnov A, Kudryavtsev A, Lahr DJG, Brown MW (2017) Between a pod and a hard test: The deep evolution of amoebae. Mol Biol Evol **34**:2258–2270

Katoh K, Standley DM (2013) MAFFT multiple sequence alignment software version 7: improvements in performance and usability. Mol Biol Evol **30**:772–780

Kudryavtsev A (2004) Description of *Cochliopodium spiniferum* sp. n., with notes on the species identification within the genus *Cochliopodium*. Acta Protozool **43**:345–349

Kudryavtsev A, Hausmann K (2009) *Thecamoeba aesculea* n. sp. (Amoebozoa, Thecamoebidae), a terrestrial amoeba with affinities to *Th. sphaeronucleolus* (Greeff, 1891). Acta Protozool **48**:91–96

Kudryavtsev A, Smirnov A (2006) *Cochliopodium gallicum* n. sp (Himatismenida), an amoeba bearing unique scales, from cyanobacterial mats in the Camargue (France). Europ J Protistol **42**:3–7

Kudryavtsev A, Wylezich C, Pawlowski J (2011) *Ovalopodium desertum* n. sp. and the phylogenetic relationships of Cochliopodiidae (Amoebozoa). Protist **162**:571–589

Lahr DJG, Grant J, Nguyen T, Lin JH, Katz LA (2011) Comprehensive phylogenetic reconstruction of Amoebozoa based on concatenated analyses of SSU-rDNA and actin genes. PLoS ONE **6**:e22780

Michel R, Wylezich C, Hauroder B, Smirnov AV (2006) Phylogenetic position and notes on the ultrastructure of *Sappinia diploidea* (Thecamoebidae). Protistology **4**:319–325

Michel R, Müller K-D, Schmid EN, Theegarten D, Hauröder B, Corsaro D (2012) Isolation of *Thecamoeba terricola* from bark of *Platanus occidentalis* harbouring spore-forming eukaryotic endoparasites with intranuclear development. Endocytobios Cell Res **22**:37–42

Miller M, Pfeiffer W, Schwartz T (2010) Creating the CIPRES Science Gateway for inference of large phylogenetic trees. Gateway Computing Environments Workshop (GCE), IEEE :1–8

Page FC (1969) *Platyamoeba stenopodia* n. g., n. sp., a freshwater amoeba. J Protozool **16**:437–441

Page FC (1971) A comparative study of five fresh-water and marine species of Thecamoebidae. Trans Am Microsc Soc **90**:157–173

Page FC (1977) The genus *Thecamoeba* (Protozoa; Gymnamoebia). Species distinctions, locomotive morphology and protozoan prey. J Nat Hist **11**:25–63

Page FC (1983) Marine Gymnamoebae. Institute of Terrestrial Ecology, Cambridge, 54 p

Page FC (1987) The classification of 'naked' amoebae (Phylum Rhizopoda). Arch Protistenkd **133**:199–217

Page FC (1988) A New Key to Freshwater and Soil Gymnamoebae. Freshwater Biological Association, Ambleside, Cumbria. p. 66–72

Page FC (1991) Nackte Rhizopoda. In Nackte Rhizopoda und Heliozoea (Protozoenfauna Band 2). Gustav Fischer Verlag, Stuttgart, New York. p. 3–187

Page FC, Blakey SM (1979) Cell surface structure as a taxonomic character in the Thecamoebidae (Protozoa: Gymnamoebia). Zool J Linn Soc **66**:113–135

Pawlowski J, Burki F (2009) Untangling the phylogeny of amoeboid protists. J Eukaryot Microbiol **56**:16–25

Peglar MT, Nerad TA, Anderson OR (2016) *Stenamoeba polymorpha*, a new species isolated from domesticated horse *Equus ferus caballus*. J Eukaryot Microbiol **63**:698–708

Rice P, Longden I, Bleasby A (2000) EMBOSS: The European Molecular Biology Open Software Suite. Trends Genet **16**:276–277

Sawyer TK (1975) *Clydonella* n. g. (Amoebida: Thecamoebidae), proposed to provide an appropriate generic home for Schaeffer's marine species of *Rugipes*, *C. vivax* (Schaeffer, 1926) N. comb. Trans Am Microsc Soc **94**:395–400

Sawyer TK, Hnath JG, Conrad JF (1974) *Thecamoeba hoffmani* sp. n. (Amoebida: Thecamoebidae) from gills of fingerling salmonid fish. J Parasitol **60**:677–682

Schaeffer AA (1926) Taxonomy of the Amebas. Pap. Department Mar. Biol., Carnegie Inst. of Washington **24**:1–116

Shadwick LL, Spiegel FW, Shadwick JDL, Brown MW, Silberman JD (2009) Eumycetozoa = Amoebozoa?: SSUrDNA phylogeny of protosteloid slime molds and its significance for the amoebozoan supergroup. PLoS ONE **4**:e6754

Smirnov AV (1999) Re-description of *Thecamoeba munda* Schaeffer 1926 (*Gymnamoebia*, Thecamoebidae), isolated from the Baltic Sea. Europ J Protistol **35**:66–69

Smirnov AV, Brown S (2004) Guide to the methods of study and identification of soil gymnamoebae. Protistology **3**:148–190

Smirnov AV, Goodkov AV (1999) An illustrated list of basic morphotypes of Gymnamoebia (Rhizopoda, Lobosea). Protistology **1**:20–29

Smirnov AV, Chao E, Nassonova ES, Cavalier-Smith T (2011) A revised classification of naked lobose amoebae (Amoebozoa: Lobosa). Protist **162**:545–570

Smirnov AV, Nassonova ES, Chao E, Cavalier-Smith T (2007) Phylogeny, evolution, and taxonomy of vannellid amoebae. Protist **158**:295–324

Smirnov AV, Nassonova ES, Berney C, Fahrni J, Bolivar I, Pawlowski J (2005) Molecular phylogeny and classification of the lobose amoebae. Protist **156**:129–142

Stamatakis A, Hoover P, Rougemont J (2008) A rapid bootstrap algorithm for the RAxML Web servers. Syst Biol **57**:758–771

Talavera G, Castresana J (2007) Improvement of phylogenies after removing divergent and ambiguously aligned blocks from protein sequence alignments. Syst Biol **56**:564–577

Tekle YI, Williams JR (2016) Cytoskeletal architecture and its evolutionary significance in amoeboid eukaryotes and their mode of locomotion. Royal Soc Open Sci **3**:160283

Tekle YI, Wood FC (2017) Longamoebia is not monophyletic: Phylogenomic and cytoskeleton analyses provide novel and well-resolved relationships of amoebozoan subclades. Mol Phylogenet Evol **114**:249–260

Tekle YI, Gorfu LA, Anderson OR (2015) *Cochliopodium arabianum* n. sp. (Amorphea, Amoebozoa). J Eukaryot Microbiol **62**:623–628

Tekle YI, Anderson OR, Katz LA, Maurer-Alcalá XX, Cerón R, Mario A, Molestina R (2016) Phylogenomics of 'Discosea': A new molecular phylogenetic perspective on Amoebozoa with flat body forms. Mol Phylogenet Evol **99**:144–154

Tekle YI, Grant J, Anderson OR, Nerad TA, Cole JC, Patterson DJ, Katz LA (2008) Phylogenetic placement of diverse amoebae inferred from multigene analyses and assessment of clade stability within 'Amoebozoa' upon removal of varying rate classes of SSU-rDNA. Mol Phylogenet Evol **47**:339–352

Wylezich C, Walochnik J, Corsaro D, Michel R, Kudryavtsev A (2015) Electron microscopical investigations of a new species of the genus *Sappinia* (Thecamoebidae, Amoebozoa), *Sappinia platani* nov. sp., reveal a dictyosome for the first time in this genus. Acta Protozool **54**:45–51